Construction of Wendelstein 7-X—Engineering a Steady-State Stellarator

Hans-Stephan Bosch, V. Erckmann, Ralf W. T. König, Felix Schauer, Reinhold J. Stadler, and A. Werner

***Abstract*—The next step in the Wendelstein stellarator line is the large superconducting device Wendelstein 7-X (W7-X), which is currently under construction in Greifswald. Steady-state operation is an intrinsic feature of stellarators, and one key element of the W7-X mission is to demonstrate steady-state operation at reactor-relevant plasma conditions, as required for an economic fusion reactor. Such steady-state operation requires development of special technologies to be discussed in this paper.**

***Index Terms*—Construction, optimized stellarator, steady-state operation, Wendelstein 7-X (W7-X).**

I. Introduction

WENDELSTEIN 7-X (W7-X), which is currently under construction in the IPP Branch Institute in Greifswald, is a fully optimized stellarator [1]. Its optimization is based on the concept of quasi-isodynamicity [2]. The criteria to select the final magnetic configuration have been the following:

1) high-quality vacuum magnetic surfaces;
2) good finite-β equilibrium properties;
3) good MHD stability properties;
4) small neoclassical transport in the "long-mean-free-path (lmfp) regime";
5) small bootstrap fraction in the lmfp regime;
6) good collisionless alpha particle containment;
7) fabrication feasibility of modular coils.

The W7-X configuration has a fivefold symmetry and is described by a rotational transform $\iota/2\pi$ of about one $(0.72 < \iota/2\pi < 1.25)$ with low shear (i.e., a small variation of $\iota/2\pi$ across the magnetic surfaces). The major radius of the plasma is 5.5 m, the effective (i.e., averaged) minor radius is 0.55 m, and the magnetic axis is helical.

The top part of Fig. 1 shows the 3-D-shaped toroidal plasma (toroidally varying poloidal cross section), with a part of the coil system producing the corresponding confining magnetic field. Clearly visible is the pentagon shape of the torus. The actual device can therefore be set up from five identical modules. Each of those is made out of two flip-symmetric parts, so that, in fact, the device is composed of ten almost-identical half modules. A schematic view of the basic device with its main components [3] is shown in the bottom part of Fig. 1.

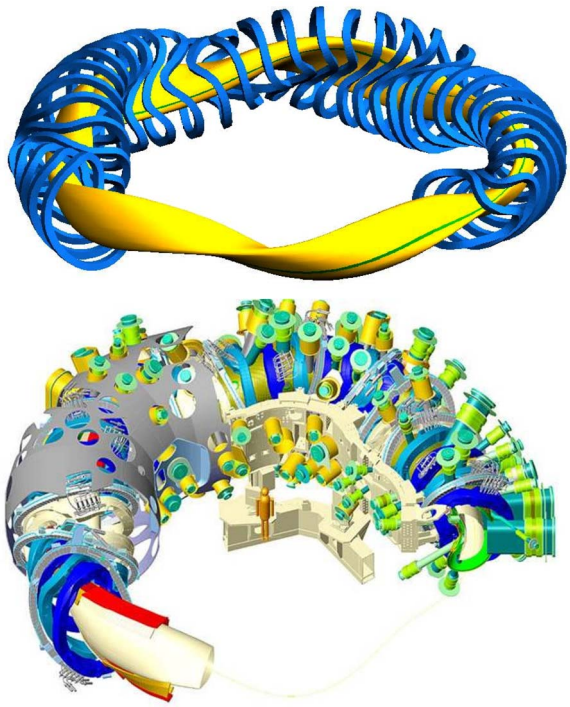

Fig. 1. (Top) Schematic view of (yellow) the toroidal plasma with a part of the 50 non-PLCs. (Bottom) Cutaway of a CAD drawing of W7-X showing (lower left) the plasma and the divertor plates, (upper right) the magnetic coils around the plasma vessel with inner support structure, and (upper left) the outer vessel.

In the first stage of its operation, W7-X will have to prove the good confinement properties predicted by numerical optimization, i.e., confinement in the range of that seen in tokamaks of comparable size. Beyond that, however, a key element of the W7-X mission is to demonstrate steady-state operation at reactor-relevant plasma conditions, as required for an economic fusion reactor. Steady-state operation is an intrinsic feature of stellarators, unlike tokamaks, where steady-state operation is still a major challenge that requires extensive research and development effort.

However, independently of the confinement scheme, steady-state operation of fusion-relevant plasmas is a complex task that is composed of both engineering and physics issues.

In this paper, the construction status of W7-X will be discussed, with special emphasis on the engineering issues of a steady-state fusion device. The main components that require special engineering to become ready for steady-state operation will be discussed in the next section. Section III will then treat the status of device assembly.

Manuscript received June 30, 2009. First published January 8, 2010; current version published March 10, 2010.

The authors are with the Max-Planck-Institut für Plasmaphysik, IPP-Euratom Association, 17491 Greifswald, Germany (e-mail: Bosch@ipp.mpg.de; Erckmann@ipp.mpg.de; ralf.koenig@ipp.mpg.de; Schauer@ipp.mpg.de; Stadler@ipp.mpg.de; Andreas.Werner@ipp.mpg.de).

Color versions of one or more of the figures in this paper are available online at http://ieeexplore.ieee.org.

Digital Object Identifier 10.1109/TPS.2009.2036918

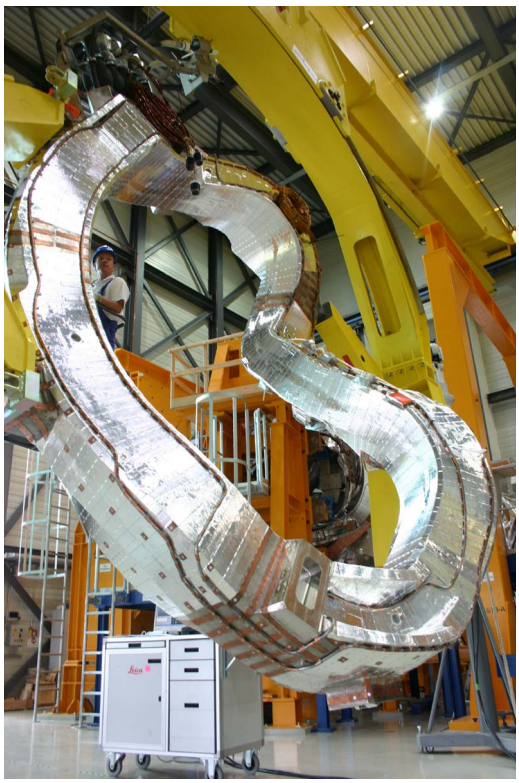

Fig. 2. Non-PLC, ready for assembly onto the plasma vessel. The coil is fixed in (yellow) the assembly handler unit.

II. "Steady-State" Components of W7-X

A. Magnetic Coil System

1) Superconducting coils: For the magnet system, the requirement of steady-state operation simply means the use of superconducting coils. This also results in the need to have a superconductive busbar system to connect the coils with each other, current leads (CLs) as transitions from the cold conductors to the room-temperature busbars and power supplies, and requires operation of a cryoplant.

The W7-X magnet system is made from 50 nonplanar coils (non-PLCs) of five different types that set up the basic confining field and from 20 PLCs (two different types) that allow for a variation of the magnetic-field configuration.

The non-PLCs (see Fig. 2) have been manufactured by a German–Italian consortium of Babcock Noell and Ansaldo Supercoductors [4]. The winding pack contains 108 windings of a NbTi cable within an Al-alloy conduit that allows He cooling through the voids between the strands of the cable. For one non-PLC, six lengths of the conductor have to be used, connected in series by low-resistance joints (< 1 nΩ) that are also used as inlets/outlets of supercritical He for superconductor cooling. The electrical insulation in this region, i.e., at the exit of the cables from the winding pack and around the interlayer joints, has turned out to be a particularly difficult area. Paschen tests, i.e., high-voltage tests at different vacuum pressure levels, have been proven to be a very effective tool for testing the quality of this insulation [5] and for unveiling problematic areas. The winding packs are embedded in cast steel casings to withstand the large electromagnetic forces resulting from the 3-D shape.

As of now, all 50 non-PLCs have been delivered. Forty nine of them have already been tested individually at CEA in Saclay, France. These cryogenic tests in full-current operation are part of the final acceptance test and have proven the expected properties for all non-PLCs [6].

The 20 PLCs, supplied by Tesla in the U.K., have casings that are made from two vertical rings and top and bottom plates bolted to them [7]. As of today, all 20 coils have already successfully completed the cryogenic tests in Saclay.

2) Magnet support system: All superconducting coils will be fixed to a central support ring (CSR). This structure is made up of ten identical welded segments that are bolted together to form a pentagon-shaped ring of five modules. The cast-steel extensions for holding the coils are welded to this ring [8]. As the coils have to be kept in their precise position, also during cooling down and operation, these fixtures have to be very rigid. The connection surfaces (flanges) on these extensions, as well as on the coils, have to be machined to a high accuracy of a few tenths of a millimeter. Eight out of the ten support-ring half modules have already been delivered, and the last two half modules are in the final stage of fabrication. The support ring will be carried by ten cryosupports that also provide the thermal barrier to the machine base in the torus hall.

Each of the 70 coils is fixed radially to the support ring in two points, where the magnetic forces (up to 4.4 MN) and bending moments (up to 450 kN $\cdot$ m) have to be taken up. To keep the coils firmly but elastically in place, a bolted solution has been developed that uses long and slender Inconel bolts and sleeves that even allow slight opening of the flanges for reduction of stresses [9].

Large electromagnetic forces also act between the non-PLCs. Therefore, they have to be supported against each other with a system that can take up the forces and moments and keep their positions to a high accuracy. On the inner side of the torus, where the distance between coils is rather small (a few centimeters) and accessibility is limited, the so-called narrow support elements (see [10]) are foreseen. These are gliding elements that can take up contact forces of up to 1.5 MN, sliding distances of up to 5 mm, and tilting of up to 1° during magnet energization. On the outboard side of the torus, the so-called lateral support elements (LSEs) are installed. These LSEs provide a rigid connection, generally made of half boxes that are welded between the neighboring coils. The crucial issue here is the proper control of welding shrinkage and distortion, which is essential to comply with the magnet system assembly tolerances. An extensive test program has been carried out to optimize the layout and welding procedures for these elements. The LSE between the modules is a bolted Inconel "bridge" which posed quite a design challenge.

3) Busbar system and CLs: To connect the coils with each other (seven groups of ten identical coils each in series) and with the CLs (which lead to the power supplies at ambient temperature), a superconducting busbar system is required (see Fig. 3). This system is being designed and manufactured by the research center Jülich (FZJ, Germany) [11]. The same conductor is used as for the coils, and the routing is done for one nonplanar and the PLC groups in a bifilar way to reduce error fields from the busbar. The design of the busbar system has been

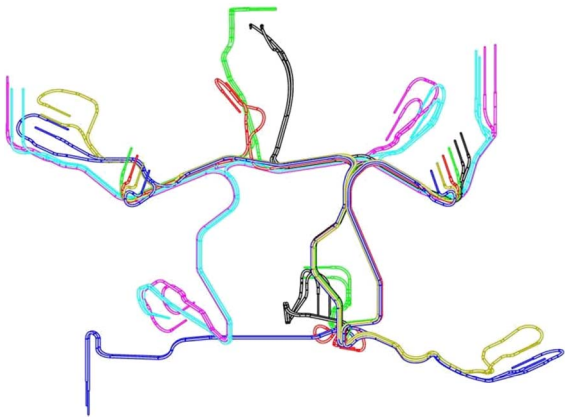

Fig. 3. Schematic view of the busbar conductors for a single magnet module of W7-X. Bifilar arrangements are used to avoid stray fields from the busbars.

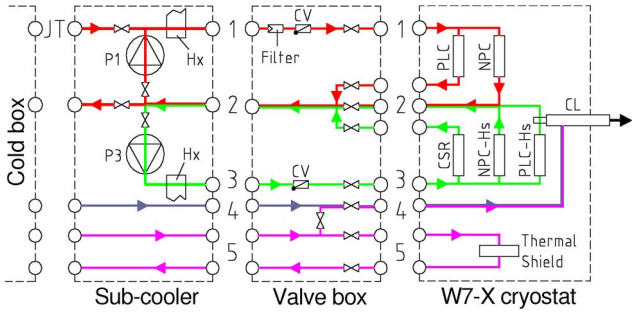

Fig. 4. Principal magnet cooling scheme. 1—Conductor supply. 2—Conductor, housing, structure, and CL auxiliary return. 3—Housing, structure, and CL auxiliary supply. 4—CL main supply. 5—Thermal shield circuit. JT—"Joule Thomson" (= main) stream from the cold box. P1 and P3—Circulation pumps. HX—Heat exchanger. CV—Check valve. PLC—Planar coil. NPC—Non-PLC. CSR—Central support ring. NPC-Hs—Housings of NPC. PLC-Hs—Housings of PLC. CL—Current leads.

finished, and manufacturing is well under way. The conductors for three modules have been delivered already, together with the corresponding supports (holders to fix the busbars to the support structure, and clamps to fix the conductors to each other).

The connection between the busbar system inside the cryostat (i.e., at about 4 K during operation and under vacuum) and the power supply lines outside the cryostat (i.e., at ambient temperature and pressure) requires 14 CLs that bridge the temperature and pressure transition. At W7-X, we have the special situation that the power supplies are located directly below the stellarator. Therefore, the CLs, mounted at the bottom of the device, have the cold end at the top, and therefore require a special layout ("bottom–up"). A detailed design for these CLs, able to carry 20 kA each and using high-temperature superconductor (HTSC) inserts, has been developed in collaboration with the research center Karlsruhe (FZK, Germany) [12]. A prototype CL is being assembled now, which will be tested under cryogenic conditions early in 2010.

4) Cooling system: The magnet system, including the structure, is cooled down to ≈4 K and kept at that level throughout the different operation regimes by a highly flexible and efficient refrigeration plant with a cooling capacity that is equivalent to about 7 kW at 4.5 K [13], [14]. Components to be supplied by individually controllable circuits are the cable-in-conduit conductors (CICCs), coil housings, the CSR, CLs, and the thermal shield (Fig. 4). The refrigerator cold box is connected to the subcooler, which, in turn, supplies via a 70-m-long multiple transfer line the valve box (VB). In the VB, the helium streams are further subdivided and distributed, again via transfer lines, to the components within the W7-X cryostat.

All the CICCs of the coils are supplied in parallel by loop 1 (Fig. 4) with supercritical He at around 4 K and 5 bar. The streams for the non-PLC and PLC sets can be controlled by valves within the VB. The distribution of the individual conductor flows within each coil set is left to the relatively high flow resistance of the cables. A filter within the VB protects the cable circuit from impurities. Another peculiarity of loop 1 is the direct supply from the Joule Thomson stream of the cold box. Circulation pump P1 is switched on if necessary, as expected during 3-T operation of the magnet system. A check valve (CV) protects the pump from the pressure wave in case of a quench.

Circuit 3 supplies the CSR and the coil housings also with 4-K He but at a lower pressure of ≈3.5 bar. This circuit is subdivided into ten individual parallel CSR loops, one per half module, and into 70 parallel loops for the coil housings. The flow resistances are balanced by one throttle valve within each of the 80 loops that is set only once except in case of abnormal component behavior during operation. Part of the PLC housing return flows is taken for additional cooling of the CL contacts. The circuit 3 return streams merge with those of loop 1 to the combined return circuit 2. The distribution of the CSR and coil housing flow is controlled within the VB by a valve in the CSR return line. Circuit 3 is exclusively driven by circulator P3 (actually two pumps in parallel), which is also quench protected by a CV within the VB.

The HTSC CLs are supplied with 50-K helium mainly from thermal shield circuit 5 that has a supply temperature of around 50 K–60 K at 14–18 bar, depending on operation conditions, and is throttled down to a pressure of 2–3 bar. In order to guarantee 50 K at the CL inlet, this flow is merged with a cold-box He stream of ≈8 K and corresponding pressure. This mixed stream is warmed up within the CL to room temperature, then expanded to atmospheric pressure, and finally fed back into the refrigerator compressor inlet stream.

The heat exchangers (HXs; see Fig. 4) downstream of the circulators reduce the supply helium temperature to minimally 3.4 K, depending on W7-X operation requirements. "HX" represents three HXs in a row that are connected to corresponding helium baths with minimal temperatures of 3.3 K, 3.8 K, and 4.4 K at corresponding pressures of 1.2, 0.66 and 0.37 bar, respectively. Both the latter subatmospheric pressure levels are provided by one centrifugal cold compressor each within the cold box.

The subcooler is provided with interfaces to be equipped with another circulation pump circuit for the divertor cryo-vacuum pumps. The corresponding circulator, transfer lines, and VB will be installed at a later state.

A special feature of the subcooler is the possibility to switch the cold-box JT stream to any one of the main cooling circuits, thus providing redundancy in case one of the circulators fails. Moreover, if needed, the refrigeration power can be boosted up to 10 kW (at 4.5-K equivalent) for several hours by expanding

liquid helium from the 10 000 LHe tank into the 3.8-K bath within the subcooler. This way, the loads can be leveled over a daily cycle.

All components of the refrigeration plant have been installed, and commissioning tests are running.

The conceptual design of the cryopiping inside the cryostat has been finished, and structural analyses have been performed [15]. The detailed design has to be adapted for each module individually due to the very tight space situation inside the cryostat. Fabrication has started, and manufacturing of the cryopipes for the first module has almost been finished.

B. In-Vessel Components

At the plasma edge, i.e., outside the closed flux surfaces, the magnetic configuration of W7-X forms an $m = 5$-island structure to be used as an island divertor to control the power and particle exhaust from W7-X [16]. According to the field structure described earlier, the divertor will also have a fivefold symmetry, i.e., it will be composed of ten units—five on the top and five on the bottom. Each unit consists of 12 target modules. This system has been designed for steady-state operation at the full electron cyclotron resonance heating (ECRH) power of 10 MW and for 10-s pulses of 15-MW NBI heating power.

The full system of the in-vessel components [17] covers an area of 265 m^2 and includes plasma-facing components, as well as cryopumps and correction coils, to modify the extent and location of the islands on the target modules, summing up to a total mass of 33.8 tons.

The plasma-facing components of the divertor are target modules, each consisting of eight to ten elements (with a horizontal and a smaller vertical target plate), and baffle modules. The highest thermally loaded parts are the actively cooled target modules with a surface area of $\sim$25 m^2 to allow a wide range of magnetic configurations. These targets will experience high power fluxes of up to 10 MW/m^2. The thermal loads are taken by flat target elements made of CuCrZr cooling structures with CFC tiles bonded to its surface. A robust bonding technology has been developed in close cooperation with the supplier, Plansee SE of Austria [18]. After a significant development effort, the technology was qualified in extensive high-heat-flux tests in the IPP GLADIS facility [19], demonstrating up to 10 000 full power cycles on the elements [20].

The baffle, adjacent to the divertor targets, prevents the neutrals in the divertor chamber from escaping into the main plasma chamber and receives lower stationary power fluxes of up to 0.5 MW/m^2. These components are built up of actively cooled CuCrZr structures with faceted graphite tiles clamped as a plasma-facing armor.

In the divertor chamber, behind the target modules, ten cryopumps are to be installed. Their design is based on the successful ASDEX Upgrade cryopump design.

Behind the baffle modules, ten control coils will be installed. Manufactured by BNG, Germany, these components will allow one to sweep the target points and to correct minor error fields.

For the remaining wall protection, two areas have to be distinguished, which require different technical solutions. The wall protection is subjected to neutral particles and plasma radiation. In higher loaded areas, on the inboard side and closer to the plasma, heat shields with clamped carbon tiles, similar to the baffles, are installed. These are designed for a heat flux of up to 0.3 MW/m^2. In the less loaded areas, steel panels will be installed, which are designed for power fluxes of up to 0.2 MW/m^2. These panels use a quilt technology to form the cooling circuits and are produced by an industrial team lead by DWE, Germany.

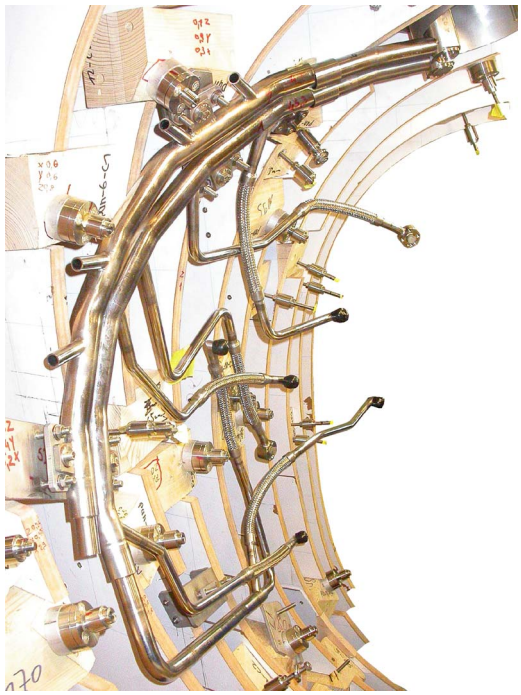

Fig. 5. Prototype cooling circuit during installation in the wooden plasma vessel mock-up.

The supply of the coolant for the components is made by a pipework of 4.5-km length. The 170 individual circuits are arranged between the in-vessel components and plasma vessel wall. The supply of the cooling water into the plasma vessel is achieved by 80 plug-ins in the supply ports. They connect the external supply lines with the internal pipe work. Fig. 5 shows a fully equipped cooling-circuit prototype during installation into a wooden plasma vessel segment mock-up.

Some diagnostic ports will be protected by panel-type port liners, and the ports for the NBI and diagnostic injector will be protected by port liners, using a technology that is similar to that of the baffles.

The design and manufacturing of the in-vessel components is well under way. The control coils were delivered to Greifswald in 2008. Over 60% of the wall protection elements have been manufactured, and the assembly of the first cooling circuits has started.

The work on an inertially cooled test divertor [21], to be installed in the first experimental phase, is running, and the design of the high-heat-flux divertor modules is going on in parallel. A prototype of a target module was tested successfully and has verified the layout. The parts of the cryopumps are available, although the pumps will be installed only later, for the second experimental phase.

C. ECRH System

The ECRH system for W7-X is being developed and built by the German research center Karlsruhe (FZK) as a joint project with IPP and IPF Stuttgart in the "Project Microwave Heating for W7-X" (PMW) being responsible for the entire ECRH system for W7-X. This ECRH system [22] has been designed for a microwave power of 10 MW in continuous-wave operation (30 min) at 140 GHz, which is resonant with the W7-X magnetic field of 2.5 T. It consists of ten gyrotrons with 1-MW power each, a low-loss quasi-optical transmission line, and a versatile in-vessel launching system. It also supports the operation of W7-X at reduced magnetic field because the gyrotrons can be tuned to 103.6-GHz radiation emission with about half the output power. This is of particular importance during the commissioning phase of W7-X and for confinement studies.

1) W7-X gyrotrons: The development of steady-state gyrotrons with output power in the megawatt range is still a subject of worldwide R&D efforts, mainly driven by the needs of W7-X and ITER.

The development of W7-X gyrotrons started in 1998 in cooperation with companies in the EU and the U.S. The design approach chosen for this development includes single-stage collector depression to enhance the efficiency and to relax the collector loading. To simplify the design, this gyrotron has no control anode. The collector is at ground potential, the cathode voltage has negative polarity, and the depression voltage (cavity and body) is positive. The output vacuum window uses a single (water-cooled) disk of chemical-vapor-deposited diamond with a diameter of 106 mm, a window aperture of 88 mm, and a thickness of 1.8 mm, corresponding to four half wavelengths.

After the successful completion of gyrotron R&D in the EU [23], the first-out-of-seven-series gyrotrons (SN1) had been delivered by Thales Electron Devices (TED) in 2005 (see Fig. 6). In the same year also, the prototype gyrotron from CPI was delivered [24]. Both gyrotrons have been tested at FZK and IPP. All the specifications were met, and no specific limitations were observed during the acceptance test. Both gyrotrons were operated for 30 min at output-power values of 900 kW (CPI gyrotron) and 920 kW (TED gyrotron), respectively, measured after transmission over 25 m. In order to keep the warranty, the SN1 gyrotron was sealed, while the two prototype gyrotrons were routinely used for the experiments. The next series gyrotrons showed, however, a different behavior with respect to parasitic oscillations excited in the beam-tunnel region, resulting in an excessive heating of the beam-tunnel components. This has limited the steady-state output power of these gyrotrons. Therefore, it was agreed with TED to stop the series production until mid-2009 and focus the activities on a coordinated beam-tunnel R&D to overcome the problems and to arrive at a more robust beam tunnel, which suppresses the excitation of parasitic oscillations more efficiently. This development is running smoothly.

2) Transmission system: The transmission line consists of single-beam-waveguide (SBWG) and multibeam-waveguide (MBWG) elements. For each gyrotron, a beam-conditioning assembly of five single-beam mirrors is used. Two of these mirrors match the gyrotron output to a Gaussian beam with the correct beam parameters, and two others are used to set the appropriate polarization needed for the optimum absorption of radiation in the plasma. A fifth mirror directs the beam to a plane mirror array, the beam-combining optics, which is situated at the input plane of an MBWG. This MBWG is designed to transmit up to seven beams (five 140-GHz beams plus additional spare channels) from the gyrotron area (entrance plane) to the stellarator hall (exit plane). At the output plane of the MBWG, a mirror array separates the beams again and distributes them via CVD-diamond vacuum barrier windows to individually movable antennas (launchers) in the torus. Long-distance transmission is provided by two symmetrically arranged MBWGs and has been simulated and tested by transmitting the high-power beams halfway in the forward direction and then back via the reflectors to the dummy load. Total losses of about 3% were measured over a total length of about 40 m. These measured total losses are in good agreement with the calculations and previous low-power measurements. This result confirms the high quality of the quasi-optical concept for high-power long-distance transmission.

Fig. 6. First series gyrotron at IPP.

3) HV systems: For the operation of gyrotrons with a depressed collector, a precisely controlled beam acceleration voltage is necessary, which is supplied by the body-voltage modulator. The beam current of the gyrotrons is controlled by the cathode heater supply, which is at cathode potential (about −55 kV). In case of arcing inside the gyrotron, a thyratron crowbar protects the tubes from being damaged. The body-voltage modulators and the protection units were designed by and built at IPF Stuttgart. All ten systems are now installed at W7-X and are ready for operation. An additional protection unit was integrated to enable the exact location of the source of a fault in case of malfunction of the gyrotron.

4) In-vessel components: The ECRH system for W7-X must provide plasma start-up and operation at full performance. The plasma start-up will be initiated by ECRH at the resonant magnetic-field strength for both operating frequencies at 105 and 140 GHz. The control of the rotational transform profile during the density buildup requires a highly flexible launching and power control system. As soon as the plasma density approaches the X2 cutoff density, a well-controlled transition from the strongly absorbed second-harmonic extraordinary-mode (X2) to a multipass second-harmonic ordinary-mode (O2) heating scenario must be performed. The key elements are the four front-steering ECRH antennas in the outboard midplane ports. All parts of the antennas are expected to experience a high-power loading by either direct microwave irradiation, in particular the mirrors and diamond vacuum windows, or by strong microwave stray radiation at the screening and support elements. Therefore, all components require active cooling and/or screening. The design of the antennas was frozen after successful tests of several critical subcomponents. Two out of four plug-in antennas modules have been completed, and tests are presently performed.

D. Diagnostics

The step being taken in W7-X toward quasi-steady-state operation poses a significant number of new challenges regarding the development of diagnostics [25]. With 10 MW of ECRH power being available for pulses of up to 30-min duration, and the duration of the discharge only being limited by the heat capacity of the cooling-water reservoir, all in-vessel diagnostic components are being exposed quasi-continuously to thermal loads of 50–100 kW/m^2 from radiation alone [26]. Some diagnostics, like the soft X-ray multicamera tomography system (XMCTS) and the in-vessel diamagnetic loops that are mounted onto the plasma vessel wall, need also to be protected against convective loads of up to 500 kW/m^2 by an actively cooled heat shield [27]. The high heat loads make it necessary to develop actively water-cooled plasma-facing optical components like windows [28] and mirrors, as well as water-cooled shutters [27], to protect some of these components during long-pulse operation from getting severely contaminated with carbon deposits. Furthermore, *in situ* cleaning techniques, like heating the optical components to elevated temperatures over night or during weekends [25], [26], and *in situ* intensity calibration techniques have to be developed. For the in-vessel retroreflectors being developed for the multichannel interferometer and the polarimeter, it is presently not known whether they will be mostly affected by deposition or erosion. A rather similar situation exists for many plasma-facing optical components in ITER. For this reason, in W7-X, the most erosion-stable material, molybdenum, is going to be used.

One of the most critical diagnostic items for steady-state operation of W7-X will be the combined infrared/visible divertor observation endoscopes [29], [30] that need to ensure that none of the targets of the ten discrete divertor modules is ever exposed to excess heat loads that could easily destroy them. These systems are designed such that the entrance pupil of their optics is lying inside an $\sim$5-mm observation pinhole inside a water-cooled stainless-steel plate facing the plasma. In this way, the transmission losses of the first mirror by the buildup of soft a:C-H layers can be minimized for such systems that, for machine protection reasons, need to be operable at all times without any interruption, i.e., no shutter may be closed during plasma operation. As has been observed in Tore Supra, redeposited carbon material across the divertor surfaces and, in particular, near the stress-relieving cuts in the divertor target material can cause major problems for the derivation of carbon tile temperatures near the interlayer to the CuCrZr cooling structure, which, at no time, may exceed 475 °C. The required spatial resolution of the IR system of less than 10 mm across each 4-m-long divertor can only be achieved by using two microbolometer cameras per system. This is due to the high diffraction limit in the wavelength region of $\sim$10 μm.

An area in which basically no prior knowledge from other fusion devices exists is the shielding of various diagnostics, in particular during high-density operation, from high levels of ECRH stray radiation. Near the cutoff densities of the X2 mode (1.25×10^{20} m^{-3}) and during O2-mode (up to 2.5×10^{20} m^{-3}) and OXB-mode operation, ECRH stray-radiation levels vary toroidally from 200 kW/m^2 in the launching plane to about 50 kW/m^2 at the opposite side of the torus. The tests in our specially set-up ECRH stray-radiation test chamber have already shown that great care needs to be taken, e.g., to properly shield the in-vessel magnetic diagnostic components to prevent overheating of the wires of the diamagnetic loops, the Rogowski or the Mirnov coils, and any other in-vessel cabling. Shielding wire meshes were found to be not suitable because they are heated to high temperatures by stray radiation. Also, observation windows, as well as many types of ceramics, absorb significant amounts of stray radiation, making shielding or efficient cooling essential.

It can be seen from the previous discussion that a major part of any diagnostic development for quasi-continuously operating nuclear fusion devices needs to be invested into making the diagnostics fit to survive in the rather hostile environment.

E. Control System

The steady-state operation of high-performance fusion plasmas can be enabled only by an intelligent control system that can drive the plasma into favorable states while taking care of the technical load limits of the first wall and divertor components. In steady-state reactor-relevant scenarios, control loops with very long time constants, like L/R or thermal time constants, pose a challenge for plasma control [31]. The W7-X system comprises several major components, namely, the steady-state data-acquisition system, the device control system with time-variable configuration parameters, and an automated data analysis system that allows for the integration of theory models. A major requirement on the data acquisition and control system is the permanent full documentation of discharges and monitoring of the machine states, with the latter running 24 h a day.

The steady-state data-acquisition system [32] has to treat a permanent data flow with transfer rates on the order of several gigabytes per second, which is demanding even for modern

network and storage technologies. It stores the data directly and, in a well-structured format, into an object database. The total amount of data per long-pulse discharge is expected to be on the order of several terabytes. Furthermore, a significant fraction of the storage is required for the interdischarge data archiving of device-state monitoring.

The control system foreseen for W7-X has to provide three different systems, namely, the safety control system, operational management, and real-time control of the plasma [33]. It is hierarchically structured in a way that each local component, such as coil power supplies, heating and cooling systems, diagnostics, and so on, has its own local control system (LCS). For commissioning and tests, these LCSs are operated autonomously. For operation of W7-X, all these components will be controlled by the central control system (CCS), which coordinates the activities of the subordinated LCS [33]. LCS and CCS consist of an operational management and a real-time control system, with the latter being supervised by the operational management itself. The real-time plasma control provides control states in temporal segments containing control parameters for LCS and CCS, which can be varied in a flexible way during the discharge. By this complete discharge, scans become feasible in single experimental runs. The safety system works independently and consists again of local units for each component, and a central safety system controlling the safety of the full system.

The analysis and modeling framework, required for the plasma-physics-driven control, will be based on service-oriented architectures in which plasma models and data analysis components are exposed as services running on distributed computing nodes. At present, grid-computing middleware is under investigation with respect to suitability, quality of service, scalability, and other requirements. It is planned to use this middleware for the coupling between distributed high-performance computing and the real-time control system.

This data-acquisition and control system for W7-X is under development, and as a system test, a first prototype is currently operated on the small WEGA stellarator in Greifswald [34]. The further development of the W7-X control system will be based on the experiences from this prototype.

III. Status of Construction

The development and manufacturing of most of the components of the basic device have been finished, except for those components where the detail design and fabrication run in parallel to the assembly, i.e., the components in the cryostat like cryopiping and thermal insulation of the outer vessel. Therefore, the main focus of the construction of W7-X has shifted from component manufacturing to the assembly of the device, which will be described in the following paragraphs.

At present, four out of the five modules are in the assembly process, which is performed on a sequence of assembly rigs [35]. On the first of these modules that is presently on assembly rig III, the busbar conductors have been assembled, and the last cryopipes are presently being mounted. Due to the narrow installation space, as mentioned earlier, the design of these pipes requires several iteration cycles of design and collision control, making this process even more time consuming than expected. Fig. 7 shows the narrow assembly space using the example of the CSR with busbars and cryopipes. At present, the joints between the busbars and coil conductors are assembled.

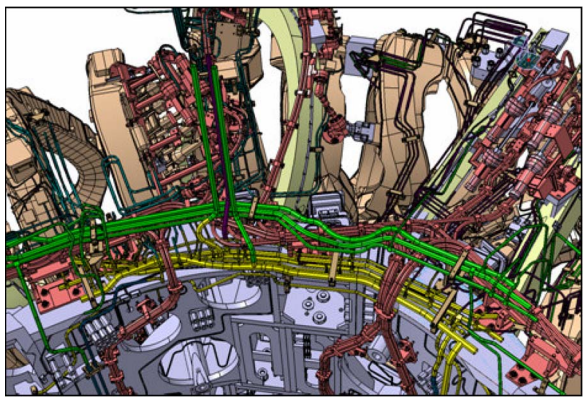

Fig. 7. CAD view of the CSR with (brown) some coils and busbars and (yellow, green, and black) cryopipes, illustrating the very tight assembly space inside the cryostat.

The second module is presently being equipped with the first cryopipes on a temporary assembly rig, while on rig II, the half modules of the third module are assembled. The half modules of the CSR have been connected with shear bolts, the vacuum vessel sectors have been welded, and the intercoil supports have been completed. The half modules of the fourth module are being assembled on a routine basis.

At present, the first module of the outer vessel [36] is being equipped with thermal insulation. Due to the very tight space inside this cryostat, also the detailed design of thermal insulation had to be subjected to an iterative collision control and design process, thereby delaying manufacturing and assembly. Therefore, the installation of the first module into the outer vessel had to be shifted by about two months. In the spring of 2010, the assembly of the first ports is scheduled to start.

IV. Summary and Outlook

For the construction of the steady-state stellarator W7-X, several components had to be further developed with regard to the steady-state requirements. These developments have been concluded successfully. As of now, the main tasks of the project are concentrated on the assembly of the device. Some of the assembly steps are performed on a routine basis by now, but there are still many assembly steps ahead that have been developed but have not yet been performed. Therefore, the schedule still bears some uncertainty for the technical risks, particularly concerning these new processes.

The general schedule for the construction of W7-X foresees the conclusion of assembly and the start of commissioning for the summer of 2014.

References

[1] J. Nührenberg, W. Lotz, P. Merkel, C. Nührenberg, U. Schwenn, E. Strumberger, and T. Hayashi, "Overview on Wendelstein 7-X theory," *Trans. Fusion Technol.*, vol. 27, p. 71, 1995.

[2] S. Gori, W. Lotz, and J. Nührenberg, "Quasi-isodynamic stellarators," in *Theory of Fusion Plasmas*. Bologna, Italy: SIF, 1996, p. 335.

[3] H.-S. Bosch, "Wendelstein 7-X—A technology step towards Demo," *Plasma Fusion Res.*, vol. 5, S1002, Mar. 2010, to be published.
[4] C. Sborchia, J. Baldzuhn, J. H. Feist, K. Riße, T. Rummel, H. Viebke, and M. Wanner, "Progress in the design, manufacture and testing of the W7-X superconducting magnets," *IEEE Trans. Appl. Supercond.*, vol. 16, no. 2, pp. 848–851, Jun. 2006.
[5] H. Scheller, H. P. Langenberg, M. Kühnberg, J. Baldzuhn, B. Petersen-Zarling, D. Gustke, and H. Fillunger, "Paschen testing on W7-X coils and components in the BNN test facility," *IEEE Trans. Appl. Supercond.*, vol. 16, no. 2, pp. 759–762, Jun. 2006.
[6] J. Baldzuhn, "Cold test of the superconducting coils for the stellarator for W7-X," *IEEE Trans. Appl. Supercond.*, vol. 18, no. 2, pp. 509–512, Jun. 2008.
[7] H. Viebke, T. Rummel, K. Riße, R. Schroeder, and R. Winter, "Fabrication of the planar coils for Wendelstein 7-X," *Fusion Eng. Des.*, vol. 75–79, pp. 201–205, Nov. 2005.
[8] A. Benito, D. Goitia, E. Casado, M. Andreres, E. Vázquez, M. Fajardo, C. Palacios, A. Cardella, D. Pilopp, L. Giodarno, and G. Di Bartolo, "Manufacturing of the coil support structure for W7-X," *Fusion Eng. Des.*, vol. 82, no. 5–14, pp. 1579–1583, Oct. 2007.
[9] A. Dudek, A. Benndorf, V. Bykov, S. Cardella, C. Damiani, A. Dübner, W. Dänner, M. Gasparotto, T. Höschen, and G. Matern, "Tests of critical bolted connections of the Wendelstein 7-X coils," *Fusion Eng. Des.*, vol. 82, no. 5–14, pp. 1500–1507, Oct. 2007.
[10] J. Reich, A. Cardella, U. Nielsen, R. Krause, H. Jenzsch, M. Bednarek, R. Kairys, G. Sobisch, and B. Vosslamber, "Manufacture of inter-coil support-elements of the W7-X magnet system," in *Proc. 22th IEEE Symp. Fusion Eng.*, Albuquerque, NM, 2007, pp. 1–4.
[11] M. Sauer, B. Giesen, A. Charl, R. Schick, S. Brons, A. Panin, H. Reimer, W. Tretter, M. Schumacher, R. Caspers, and W. Schalt, "Design and construction of the superconducting bus system for the stellarator W7-X," *Fusion Eng. Des.*, vol. 82, no. 5–14, pp. 1460–1466, Oct. 2007.
[12] W. H. Fietz, R. Heller, A. Kienzler, and R. Lietzow, "High temperature superconductor current leads for Wendelstein 7-X and JT-60SA," *IEEE Trans. Appl. Supercond.*, vol. 19, no. 3, pp. 2202–2205, Jun. 2009.
[13] F. Schauer, H. Bau, Y. Bozhko, C. P. Dhard, M. Nagel, M. Pietsch, and S. Raatz, "Kryotechnik fuer die Supraleiterspulen des Wendelstein 7-X," *KI Luft- und Kaeltetechnik*, vol. 4, p. 124, 2005.
[14] A. Kuendig, C. P. Dhard, S. Raatz, and H. Bau, "Progress report of the cryo-plants for Wendelstein-7X," in *Proc. 22nd Int. Cryog. Eng. Conf.*, Seoul, Korea, 2008.
[15] A. Dübner, D. Zacharias, M. Nagel, V. Bykov, F. Schauer, and M. Ihrke, "Structural analysis of the W7-X cryogenic pipe system," *Fusion Eng. Des.*, vol. 84, no. 2–6, pp. 684–697, Jun. 2009.
[16] H. Renner, D. Sharma, J. Kißlinger, J. Boscary, H. Grote, and R. Schneider, "Physical aspects and design of the Wendelstein 7-X divertor," *Fusion Sci. Technol.*, vol. 46, no. 2, pp. 318–326, 2004.
[17] R. Stadler, A. Vorköper, J. Boscary, A. Cardella, F. Hurd, C. Li, B. Mendelevitch, A. Peacock, and H. Pirsch, "The in-vessel components of the experiment Wendelstein 7-X," *Fusion Eng. Des.*, vol. 84, no. 2–6, pp. 305–308, Jun. 2009.
[18] J. Boscary, H. Greuner, T. Friedrich, H. Traxler, B. Mendelevitch, B. Böswirth, J. Schlosser, M. Smirnow, and R. Stadler, "Pre-series and testing route for the serial fabrication of W7-X target elements," *Fusion Eng. Des.*, vol. 84, no. 2–6, pp. 497–500, Jun. 2009.
[19] H. Greuner *et al.*, "High heat flux facility GLADIS: Operational characteristics and results of W7-X pre-series target tests," *J. Nucl. Mater.*, vol. 367–370, pp. 1444–1448, Aug. 2007.
[20] J. Boscary, B. Böswirth, H. Greuner, M. Missirlian, B. Schedler, K. Scheiber, J. Schlosser, and B. Streibl, "Results of the examinations of the W7-X pre-series target elements," *Fusion Eng. Des.*, vol. 82, no. 15–24, pp. 1634–1638, Oct. 2007.
[21] A. Peacock, H. Greuner, F. Hurd, J. Kißlinger, R. König, B. Mendelevitch, R. Stadler, F. Schauer, R. Tivey, J. Tretter, C. von Sehren, and M. Ye, "Progress in the design and development of a test divertor (TDU) for the start of W7-X operation," *Fusion Eng. Des.*, vol. 84, no. 7–11, pp. 1475–1478, Jun. 2009.
[22] V. Erckmann, P. Brand, H. Braune, G. Dammertz, G. Gantenbein, W. Kasparek, H.P. Laqua, H. Maassberg, N.B. Marushchenko, G. Michel, M. Thumm, Y. Turkin, M. Weißgerber, and A.Weller, "Electron cyclotron heating for W7-X: Physics and technology," *Fusion Sci. Technol.*, vol. 52, no. 2, pp. 291–312, Aug. 2007. W7-X ECRH TEAM.
[23] G. Dammertz, S. Alberti, A. Arnold, E. Borie, V. Erckmann, G. Gantenbein, E. Giguet, R. Heidinger, J. P. Hogge, S. Illy, W. Kasparek, K. Koppenburg, M. Kuntze, H. P. Laqua, G. LeCloarec, Y. LeGoff, W. Leonhardt, C. Lievin, R. Magne, G. Michel, G. Muller, G. Neffe, B. Piosczyk, M. Schmid, K. Schworer, M. K. Thumm, and M. Q. Tran, "Development of a 140-GHz 1-MW continuous wave gyrotron for the W7-X stellarator," *IEEE Trans. Plasma Sci.*, vol. 30, no. 3, pp. 808–818, Jun. 2002.
[24] K. Felch, M. Blank, P. Borchard, P. Calahan, S. Cauffman, T. S. Chu, and H. Jory, "Recent ITER-relevant gyrotron tests," *J. Phys., Conf. Ser.*, vol. 25, pp. 13–23, 2005.
[25] H.-J. Hartfuss, R. König, and A. Werner, "Diagnostics for steady state plasmas," *Plasma Phys. Control. Fusion*, vol. 48, no. 10, pp. R83–R150, Sep. 2006.
[26] T. Eich and A. Werner, "Numerical studies on radiative heat loads to plasma-facing components for the W7-X stellarator," *Fusion Sci. Technol.*, vol. 53, no. 3, pp. 761–779, Apr. 2008.
[27] R. König, "Diagnostic developments for quasicontinuous operation of the Wendelstein 7-X stellarator," *Rev. Sci. Instrum.*, vol. 79, no. 10, p. 10F 337, Oct. 2008.
[28] R. König, K. Grosser, D. Hildebrandt, O. V. Ogorodnikova, C. V. Sehren, and T. Klinger, "Development of an actively cooled periscope head suitable for divertor observation during quasi-continuous operation of the W7-X stellarator," *Fusion Eng. Des.*, vol. 74, no. 1–4, pp. 751–755, Nov. 2005.
[29] J. Cantarini, "Optical design study of an infrared visible viewing system for Wendelstein 7-X divertor observation control," *Rev. Sci. Instrum.*, vol. 79, no. 10, p. 10F 513, Oct. 2008.
[30] R. König, D. Hildebrandt, T. Hübner, F. Klinkhamer, K. Moddemeijer, and W. Vliegenhart, "Optical design study for divertor observation at the stellarator W7-X," *Rev. Sci. Instrum.*, vol. 77, no. 10, p. 10F 121, Oct. 2006.
[31] A. Werner, A. Dinklage, G. Kühner, H. Maaßberg, J. Schacht, J. Svensson, U. von Toussaint, and Y. Turkin, "Integrated software development for Wendelstein 7-X," in *Proc. 21st IAEA Fusion Energy Conf.*, Chengdu, China, 2006.
[32] P. Heimann, S. Heinzel, C. Hennig, H. Kühntopf, H. Kroiss, G. Kühner, J. Maier, J. Reetz, and M. Zilker, "Status report on the development of the data acquisition system of Wendelstein7-X," *Fusion Eng. Des.*, vol. 71, no. 1–4, pp. 219–224, Jun. 2004.
[33] J. Schacht, H. Laqua, M. Lewerentz, I. Müller, S. Pingel, A. Spring, and A. Wölk, "Overview and status of the control system of Wendelstein 7-X," *Fusion Eng. Des.*, vol. 82, no. 5–14, pp. 988–994, Oct. 2007.
[34] J. Schacht, T. Bluhm, U. Herbst, C. Hennig, S. Heinrich, G. Kühner, E. Köster, H. Laqua, M. Lewerentz, M. Marquardt, C. Meyer, I. Müller, S. Pingel, J. Sachtleben, A. Spring, A. Werner, and A. Wölk, "Overview and status of the prototype project for Wendelstein 7-X control system," *Fusion Eng. Des.*, vol. 84, no. 7–11, pp. 1723–1728, 2009.
[35] L. Wegener, "Status of Wendelstein 7-X construction," *Fusion Eng. Des.*, vol. 84, no. 2–6, pp. 106–112, Jun. 2009.
[36] T. Koppe, A. Cardella, J. Reich, B. Missal, B. Hein, R. Krause, H. Jenzsch, D. Hermann, M. Schrader, P. van Eeten, G. Di Bartolo, F. Leher, A. Binni, J. Segl, R. Camin, L. Giordano, B. Egloff, J. Ridzewski, and G. Corniani, "Manufacturing and assembly status of main components of Wendelstein 7-X cryostat," in *Proc. 23rd IEEE Symp. Fusion Eng.*, San Diego, CA, 2009.

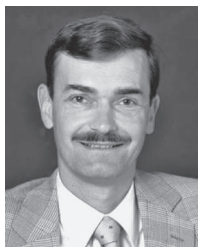

Hans-Stephan Bosch received the Dipl.-Phys. degree from Ludwigs-Maximilians University Munich, Germany, in 1983, the Dr. rer. nat. degree from the Technical University, Munich, in 1986, and the Habilitation degree from Humboldt University, Berlin, Germany, in 2000.

He became a Lecturer with Greifswald University, Greifswald, Germany, in 2008. He is currently an Associate Director (Coordination) of the Wendelstein 7-X project at Max-Planck-Institut für Plasmaphysik, Greifswald. His research interests are plasma edge and divertor physics.

V. Erckmann, photograph and biography not available at the time of publication.

Ralf W. T. König received the Dipl.-Phys. and Dr. rer. nat. degrees from Ruhr-University Bochum, Bochum, Germany, in 1984 and 1989, respectively.

From 1989 to 1998, he was an Experimental Physicist for EURATOM at JET Joint Undertaking, Culham, U.K. In 1998, he joined the Max-Planck-Institut für Plasmaphysik, Greifswald, Germany. Since 2006, he has been the Head of the W7-X Diagnostics Department and, since 2007, has also been providing physics support to the Divertor Design Team and the Deputy Leader of the Physics Division.

Felix Schauer received the M.S. degree in technical physics and the Ph.D. degree in electrical engineering from the Technical University of Graz, Graz, Austria.

He has worked in the fields of cryogenics and superconductivity and is currently the Head of the W7-X Engineering Division, Max-Planck-Institut für Plasmaphysik, Greifswald, Germany, where he has been involved in the design of major W7-X components in leading positions.

Reinhold J. Stadler received the Dipl.-Ing. (TU) degree from the Technical University, Munich, Germany, in 1989.

He is currently a Group Leader with the Department for Tokamak Scenario Development, Max-Planck-Institut für Plasmaphysik, Garching, Germany, where he is responsible for the development of the first wall of the Wendelstein 7-X project.

A. Werner, photograph and biography not available at the time of publication.